Environment International 121 (2018) 1162–1171

Contents lists available at ScienceDirect

Environment International

journal homepage: www.elsevier.com/locate/envint

Nano-metal oxides induce antimicrobial resistance via radical-mediated mutagenesis

Ye Zhang[a], April Z. Gu[b], Shanshan Xie[a], Xiangyang Li[a], Tianyu Cen[a], Dan Li[a,*], Jianmin Chen[a]

[a] Shanghai Key Laboratory of Atmospheric Particle Pollution and Prevention (LAP^3), Department of Environmental Science and Engineering, Fudan University, Shanghai 200433, China

[b] School of Civil and Environmental Engineering, Cornell University, Ithaca, NY 14853, United States

ARTICLE INFO

Keywords:
Antimicrobial resistance genes (ARGs)
Nano-metal oxides
Genic mutation
Reactive oxygen species (ROS)
SOS response

ABSTRACT

The widespread use of nanoparticles has triggered increasing concern and interest due to the adverse effects on global public health and environmental safety. Whether the presence of nano-metal oxides (NMOs) could facilitate the formation of new antimicrobial resistance genes (ARGs) via de novo mutation is largely unknown. Here, we proved that two widely used NMOs could significantly improve the mutation frequencies of CIP- and CHL-resistant *E. coli* isolates; however, the corresponding metal ions have weaker effects. Distinct concentration-dependent increases of 1.0–14.2 and 1.1–456.3 folds were observed in the resistance mutations after treatment with 0.16–100 mg/L nano-Al_2O_3 and 0.16–500 mg/L nano-ZnO, respectively, compared with those in the control. The resistant mutants showed resistance to multiple antibiotics and hereditary stability after sub-culturing for 5 days. We also explored the mechanism underlying the induction of antimicrobial resistance by NMOs. Whole-genome sequencing analysis showed that the mutated genes correlated with mono- and multidrug resistance, as well as undetected resistance to antibiotics. Furthermore, NMOs significantly promoted intracellular reactive oxygen species (ROS), which would lead to oxidative DNA damage and an error-prone SOS response, and consequently, mutation rates were enhanced. Our findings indicate that NMOs could accelerate the mutagenesis of multiple-antibiotic resistance and expanded the understanding of the mechanisms in nanoparticle-induced resistance, which may be significant for guiding the production and application of nanoparticles.

1. Introduction

Nano-metal oxides (NMOs) are attractive for numerous industrial and consumer products because of their unique catalytic activity, optoelectronic properties and antimicrobial capacity (Seabra and Duran, 2015; Liu et al., 2014). Diverse NMOs, such as nano-alumina (nano-Al_2O_3) and nano-zinc oxide (nano-ZnO), have diffused into various natural environments and even the microenvironment in vivo, which have generated great concerns about their adverse effects on human health and environmental safety (Gottschalk et al., 2009; Chalew et al., 2013; Hristozov et al., 2016). Accumulating evidence indicates the toxicological impacts of NMOs on microorganisms, algae, plants, human cells, and animals (Seabra and Duran, 2015; Chen et al., 2014). However, the impact of NMOs is still not fully understood, with one of the biggest knowledge gaps being their effects on antimicrobial resistance, which is an increasing threat to public health worldwide (Ding et al., 2016; Aruguete et al., 2013; WHO, 2014; Larsson et al., 2018).

Certain NMOs, as well as nano-metals, fullerenes, nanotubes, and macromolecular antimicrobial polymers (MAPs), have been used as broad-scale antimicrobial agents in consumer products with their assumed ability to generate reactive oxygen species (ROS) and damage the cell membrane without being toxic to the surrounding tissue in vivo (Aruguete et al., 2013; Pelgrift and Friedman, 2013). Particularly, some nanoparticles have been considered as new weapons against multidrug-resistant (MDR) infectious organisms (also known as “superbugs”), which cause worse clinical outcomes and even death (Aruguete et al., 2013; WHO, 2014). The risks of using nanoparticles as antibacterial agents have aroused growing attention, as exposure of bacteria to antimicrobial nanoparticles could lead to selective pressures that may be beneficial to emerging antimicrobial resistance (Aruguete et al., 2013; Hajipour et al., 2012). Therefore, the development and spread of antimicrobial resistance that caused by nanoparticles should be regarded as an important aspect of nanotoxicology. However, there are only a few recent studies in this area (Ding et al., 2016; Qiu et al., 2012). Qiu et al. first reported that nanoalumina could stimulate the conjugation (Qiu et al., 2012) and transformation (Ding et al., 2016) of plasmids

* Corresponding author.
E-mail address: lidanfudan@fudan.edu.cn (D. Li).

https://doi.org/10.1016/j.envint.2018.10.030
Received 24 May 2018; Received in revised form 25 September 2018; Accepted 16 October 2018
Available online 25 October 2018
0160-4120/

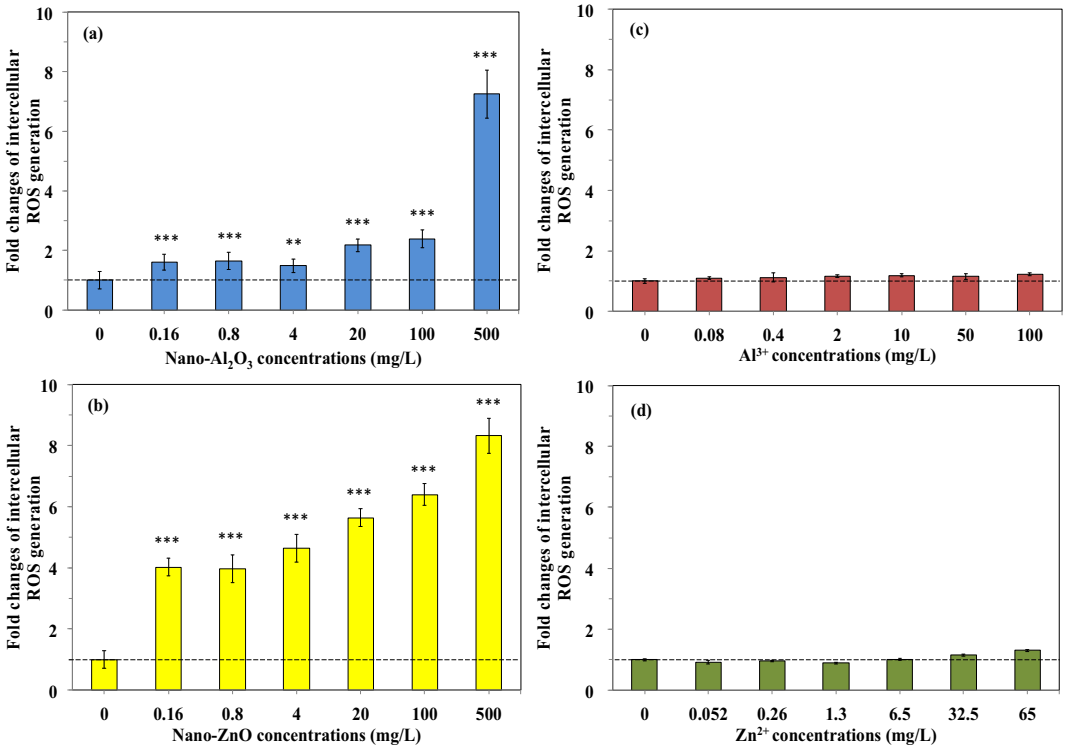

Fig. 1. ROS generation in *E. coli* induced by nano-Al_2O_3, nano-ZnO, Al^{3+}, and Zn^{2+}. Nano-Al_2O_3 and nano-ZnO had significant effects on the ROS generation in *E. coli* (ANOVA, $P < 0.05$); significant differences in the ROS generation between individual substance-exposed groups and the control (0 mg/L of substance) were tested with Independent-sample *t*-test and shown with * ($P < 0.05$), ** ($P < 0.01$), and *** ($P < 0.001$).

encoding antibiotic resistance, which may accelerate the spread of antibiotic resistance in the environment.

The development and spread of antimicrobial resistance are enhanced by the acquisition of antimicrobial resistance genes (ARGs) via de novo mutation (Andersson and Hughes, 2014; Lv et al., 2014) and horizontal transfer of ARGs (Beaber et al., 2004; Hocquet et al., 2012; Vikesland et al., 2017; Qiao et al., 2018). Specifically, genetic mutations are considered important pathways through which new ARGs, which are stable molecules encoded in the DNA, emerge, and once established, they can spread from parents to offspring or between neighboring bacterial cells by horizontal gene transfer (Andersson and Hughes, 2014).

Previous studies have indicated that resistance mutations can be stimulated by antibiotics (Zhang et al., 2011; Andersson and Hughes, 2014), disinfectants (Chapman, 2003), and disinfection by-products (DBPs) (Li et al., 2016; Lv et al., 2014) via broadly conserved cellular functions and pathways, such as those involved in oxidative stress and SOS response systems (Andersson and Hughes, 2014; Chapman, 2003; Li et al., 2016). Recent evidences suggested that the enhanced intracellular ROS production and the induction of SOS response (Baharoglu and Mazel, 2011; Baharoglu et al., 2013) can be important mechanisms involved in antimicrobial resistance via increasing the rate of mutagenesis during chromosome replication by the induction of error-prone DNA polymerases and the suppression of mismatch repair (Andersson and Hughes, 2014; Kohanski et al., 2010; Gutierrez et al., 2013). The physical, chemical, and toxic properties of NMOs were extensively studied, and previous results showed that NMOs could induce ROS-mediated cytotoxicity and DNA damage in both prokaryotic and eukaryotic cells (Seabra and Duran, 2015; Misra et al., 2012; Tong et al., 2013). Therefore, we hypothesize that NMOs can induce resistant mutagenesis by producing intracellular ROS, and triggering oxidative stress and the SOS response.

To test this hypothesis, the opportunistic pathogen *Escherichia coli* (*E. coli*) K12 was exposed to two NMOs (nano-Al_2O_3 and nano-ZnO), and the development of resistance phenotype to six widely used antibiotics was firstly evaluated. Furthermore, the mechanisms underlying the induction of resistance mutations were investigated with regard to intracellular ROS production, oxidative stress, SOS response, and genetic changes in the whole-genome. Our findings expand the understanding of the mechanisms in nanoparticle-induced antimicrobial resistance and are significant for guiding the production and application of nanoparticles.

2. Material and methods

2.1. NMOs, antibiotics and E. coli strains

Nano-Al_2O_3 (cat. no. A119404) and nano-ZnO (cat. no. Z119436) were purchased from Aladdin Reagent Inc., Shanghai, China. The characteristics of the two NMOs are listed in Table S1. The stock solutions were sterilized at 121 °C for 20 min. To avoid aggregation, the suspensions of nano-Al_2O_3 and nano-ZnO were ultrasonicated for 30 min using an ultrasonic bath before each exposure experiment. The performance of aluminum ions (Al^{3+}) and zinc ions (Zn^{2+}) were also assessed in the following experiments.

Minimal inhibition concentrations (MICs, 90% inhibition of growth) of nano-Al_2O_3, nano-ZnO, Al^{3+}, and Zn^{2+} were determined based on dose-dependent inhibitory curves of *E. coli* with treatments of various concentrations of NMOs and corresponding ions (Text S1, Fig. S1, and Table S2).

The exposure concentrations of NMOs and ions used in our study were selected not only considering the MICs determined in this study (Fig. S1, Table S2), but also considering the environmental exposure relevance based on the detected and predictive environmental concentrations (for example, in wastewater treatments: 1 mg/L–100 g/L nano-Al_2O_3 and 1 mg/L–50 mg/L nano-ZnO) (Ding et al., 2016; Zheng et al., 2011; Waseem et al., 2014), and previous studies (0–5000 mg/L nano-Al_2O_3 and 0–100 mg/L nano-ZnO) (Qiu et al., 2012; Song et al.,

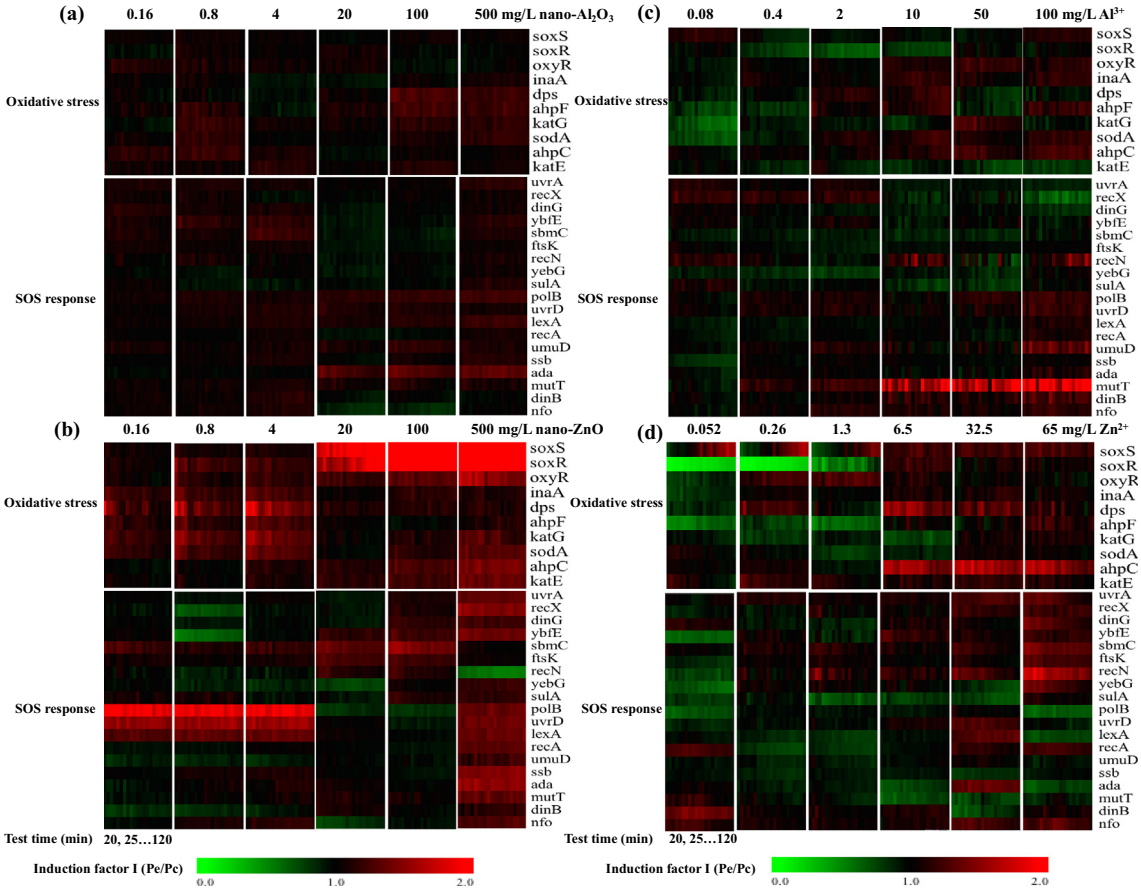

Fig. 2. Temporal gene expression profiles of target genes in recombinant *E. coli* involved in oxidative stress and SOS response by exposure to nano-Al_2O_3 (a), nano-ZnO (b), Al^{3+} (c) and Zn^{2+} (d). (X-axis) The values of Induction factor I (depicted as a green-black-red color scale. Red spectrum colors indicate up-regulated expression, while green spectrum colors indicate down-regulated expression) and monitoring time in minutes (the first time-point shown is at 20 min after exposure due to moving average). (Y-axis left) Clusters of genes. (Y-axis right) List of genes tested. (For interpretation of the references to color in this figure legend, the reader is referred to the web version of this article.)

2010; Xu et al., 2016). The tested concentrations were summarized in Table S2. The concentrations of NMOs and ions in present study chosen ranged from several- to thousands-fold below the MICs (Table S2), and represent the range of concentrations that widely present in environments, except for 500 mg/L of nano-ZnO.

The six antibiotics examined in the present study included ciprofloxacin (CIP), chloramphenicol (CHL), tetracycline (TET), gentamicin (GEN), ampicillin (AMP), and erythromycin (ERY), all of which were obtained from TCI (TCI, Shanghai, China). The detailed information on these antibiotics is listed in Table S3. The MICs of these antibiotics against the initial drug-sensitive *E. coli* K12 (MG1655) strains were also tested (shown in Table S3).

The −80 °C stock wild-type *E. coli* K12 MG1655 strain was streaked on Luria–Bertani (LB) agar plates and then incubated at 37 °C overnight. Then a single colony, which was used as the isogenic "seeds" in following experiments, was picked from LB agar plate and then incubated in 10 mL LB broth at 37 °C for 16 h with 150 rpm shaking.

2.2. Transmission electron microscope (TEM) analysis

The size, morphology of NMOs, and impact of NMOs on cell structures and morphology was evaluated by observing the interaction of NMOs and the cells via previous procedures (Qiu et al., 2012; Zhang et al., 2018), and the detailed protocols are presented in Text S2.

2.3. Measurement of intracellular ROS levels induced by NMOs

The intracellular ROS levels in the *E. coli* were assessed by staining with dye 2′,7′-Dichlorofluorescein diacetate (DCFH-DA) (Invitrogen; Carlsbad, CA). The detailed protocols and data analysis were according to our previous publications (Zhang et al., 2017, 2018) and are shown in Text S3.

2.4. Transcriptomic analysis of the impacts of NMOs on oxidative stress and SOS response pathways

The effects of the NMOs on oxidative stress and SOS response pathways, which were previously shown to contribute to resistant mutagenesis (Lv et al., 2014; Li et al., 2016), were assessed using 29 reporter strains of *E. coli* K12 MG1655 with transcriptional green fluorescent protein (GFP) fused promoters (refer to Table S4 for the list of promoters responsible for oxidative stress and SOS response genes) according to the protocols (shown in Text S4) described in our previous studies (Li et al., 2016; Gou et al., 2010).

2.5. Treatment with NMOs and corresponding ions, determination of mutation frequencies, and isolation of resistant strains

The overnight culture of the isogenic *E. coli* K12 (approximately 10^8–10^9 CFU/mL) was diluted 1:100 in 5 mL of LB broth in a 20 mL tube containing nano-Al_2O_3, nano-ZnO, Al^{3+}, and Zn^{2+} at various concentrations, along with control groups that were not exposed to the

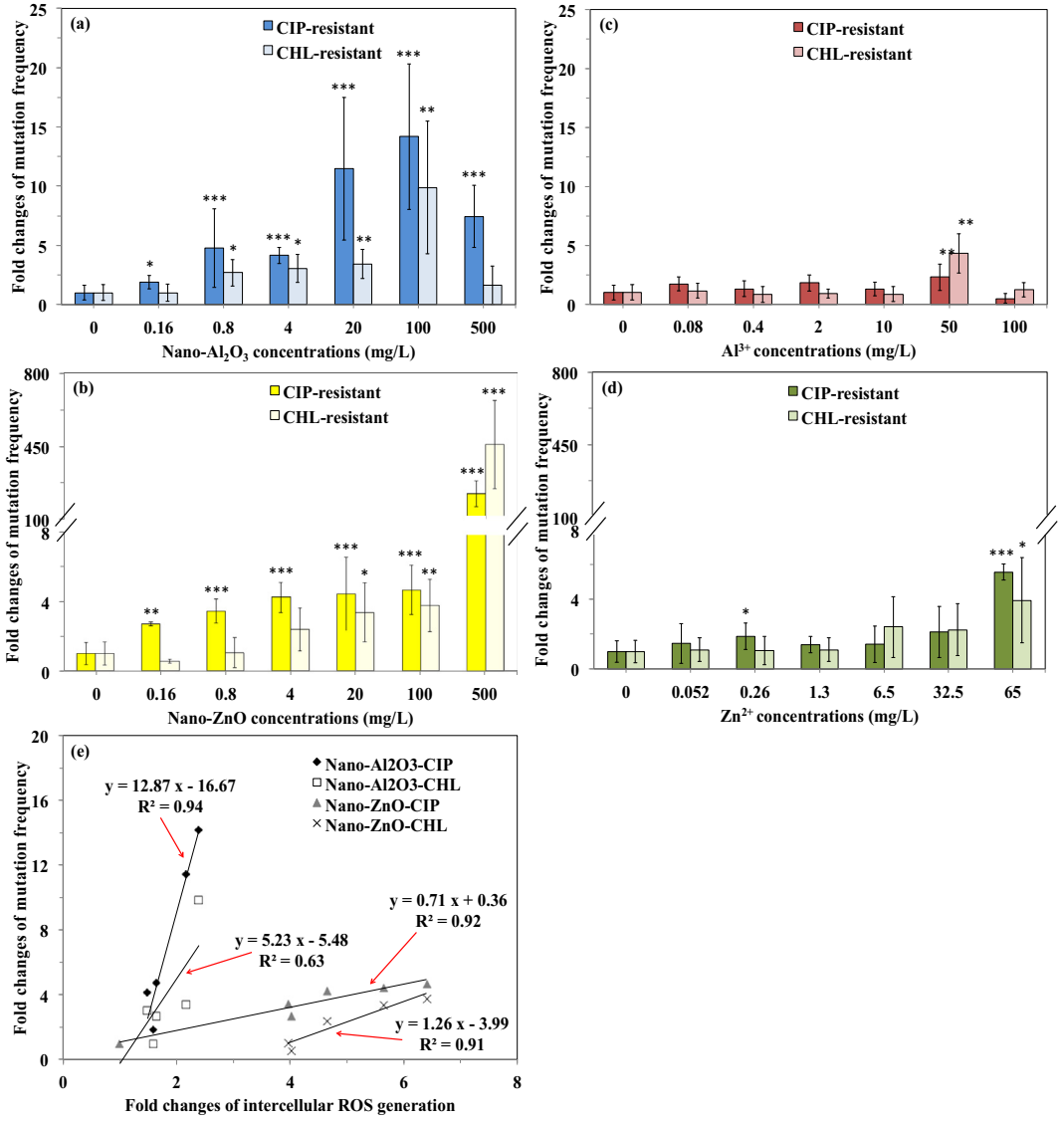

Fig. 3. Mutation frequency changes induced by NMOs and corresponding ions, and the former correlation with intracellular ROS generation. Fold changes of mutation frequency for the CIP- and CHL-resistant *E. coli* isolates by exposure to nano-Al_2O_3 (a), nano-ZnO (b), Al^{3+} (c) and Zn^{2+} (d). NMOs and corresponding ions had significant effects on fold change of mutation frequency (ANOVA, $P < 0.05$); significant differences in fold change of mutation frequency between individual NMO- or ions-exposed groups and the control (0 mg/L of NMO) were tested with Independent-sample *t*-test and shown with * ($P < 0.05$), ** ($P < 0.01$), and *** ($P < 0.001$). (e) Correlations between the fold changes of mutation frequency and the fold changes of intracellular ROS generation in *E. coli* induced by nano-Al_2O_3 and nano-ZnO described in (a) and (b).

above-mentioned chemicals. Each treatment had three replicates, and these cultures were incubated at 37 °C for 24 h with shaking at 200 rpm.

To isolate and determine the resistant mutations in the chemical-treated cultures, aliquots of each treatment were plated on LB agar plates supplemented with different antibiotics at 1 × MIC, as shown in Table S3, and incubated for 48 h at 37 °C. The multiple solution scheme (MSS) maximum-likelihood method was applied to estimate the frequency of appearance of mutated cells in each culture (Rosche and Foster, 2000). In this study, the mutation efficiency was calculated by dividing the number of mutant clones in each treatment culture by the number of total CFUs according to previous studies (Lv et al., 2014; Kohanski et al., 2010; Rosche and Foster, 2000). The total bacterial concentrations were enumerated by plating on the LB agar. The difference between the frequency of appearance of mutated cells in the treatment and that of the control were considered to account for the mutations induced by chemical treatments (Lv et al., 2014; Kohanski et al., 2010). Fold changes in the mutation frequency were determined for all treatments relative to an untreated control group. All treatments and controls were established in triplicate.

To screen the resistance phenotype of the mutant strains to six different antibiotics, at least 4 mutant clones were randomly picked from each treatment, as well as from the control groups. The above colonies were regrown in 5 mL of fresh LB medium at 37 °C for approximately 6 h and then subjected to MICs determination. MICs for the original *E. coli* K12 strain before the treatments with NMOs against the six antibiotics, as well as against each of the two NMOs, were also measured. The detailed protocol and data analysis for MICs measurements are shown in Text S1.

2.6. Hereditary stability of the resistant mutations

Hereditary stability of the acquired antibiotic resistance of the evolved mutant strains was tested for five 24-h growth cycles over a period of 5 days (Lv et al., 2014; Kohanski et al., 2010). Briefly, the mutant strains were diluted 1:100 and cultured in antibiotic-free LB broth at 37 °C for 24 h with shaking at 180 rpm. Each mutant strain had

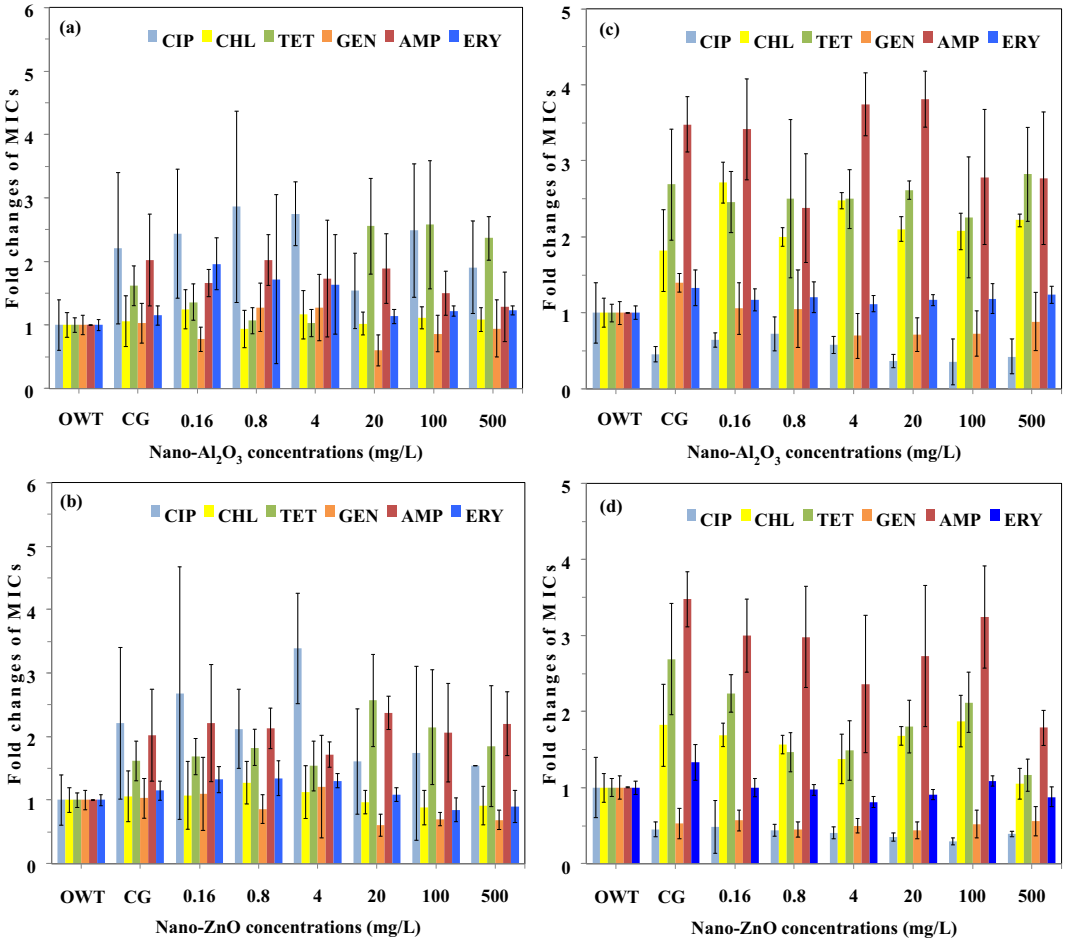

Fig. 4. Fold changes of MICs of CIP-resistant (a and b) and CHL-resistant (c and d) isolates against 6 different antibiotics induced by nano-Al_2O_3 and nano-ZnO, respectively. OWT means original wild-type (OWT) *E. coli*; CG means control group (CG). Results shown are an average of triplicates with error bar indicating standard deviation.

undergone five such rounds of growth. The MIC values were determined at the end of 5 days sub-culture and compared with the initial MIC values to verify if the antibiotic resistance phenotype was inhered and stable (Text S1).

2.7. DNA extraction, whole-genome sequencing, and data analysis

A detailed methods description of DNA extraction, whole-genome sequencing and data analysis is available in Text S5.

2.8. Statistical analysis

Each experiment in this study was conducted in triplicate. Significant differences were statistically estimated using analysis of variance (ANOVA) and an independent sample *t*-test, which was run in SPSS 16.0 for Windows (SPSS, Chicago, USA). A value of $P < 0.05$ was regarded as significant, a value of $P < 0.01$ was regarded as very significant, and a value of $P < 0.001$ was regarded as extremely significant.

3. Results and discussion

3.1. Assessment of intracellular ROS levels, oxidative stress, and SOS response induced by NMOs

To determine the effects of the NMOs on the ROS levels in *E. coli*, intracellular ROS were measured using DCFH-DA (Zhang et al., 2017). It is recognized that this dye method may not be reliable for direct quantification of ROS (Kalyanaraman et al., 2012). Therefore, in this study, the fold changes of ROS generation were used following the similar approach as suggested by others (Gupta et al., 2014; Lee et al., 2015). Both nano-Al_2O_3 and nano-ZnO induced concentration-dependent increases in intracellular ROS levels compared with those of the control groups (Fig. 1a–b). Control tests with metal ions of Al^{3+} and Zn^{2+} only led to a slight increase in ROS generation, much less than those by their corresponding NMOs (Fig. 1c–d), suggesting little contribution of metal ions to the total ROS generation, as previously reported (Misra et al., 2012; Yu et al., 2013).

In addition, TEM images showed that the cell structures of the control and tested groups exposed to 4 mg/L NMOs were intact (Fig. S2b, e, and g). However, 100 mg/L NMOs damaged the cell membranes of *E. coli* and the cytoplasm agglomerated. Additionally, parts of NMOs entered the bacterial cells (Fig. S2c and f), which might stimulate more intracellular ROS and consequently induce oxidative stress and SOS response (Qiu et al., 2012; Song et al., 2010).

The temporal transcriptional profiles of *E. coli* K12 MG1655 suggested that both NMOs and the corresponding metal ions altered the expression of genes involved in oxidative stress and SOS response pathways (Fig. 2). Particularly, nano-ZnO treatment significantly up-regulated the transcriptional expression of oxidative stress-related genes (*soxS*, *soxR*, *oxyR*, and *ahpC*) and DNA damage-inducible SOS response-related genes (*recX*, *sbmC*, *ssb*, and *ada*) (Fig. 2b). Overall, nano-ZnO induced more significant oxidative stress and SOS responses than nano-Al_2O_3. The effects of Al^{3+} and Zn^{2+} on the alteration of gene

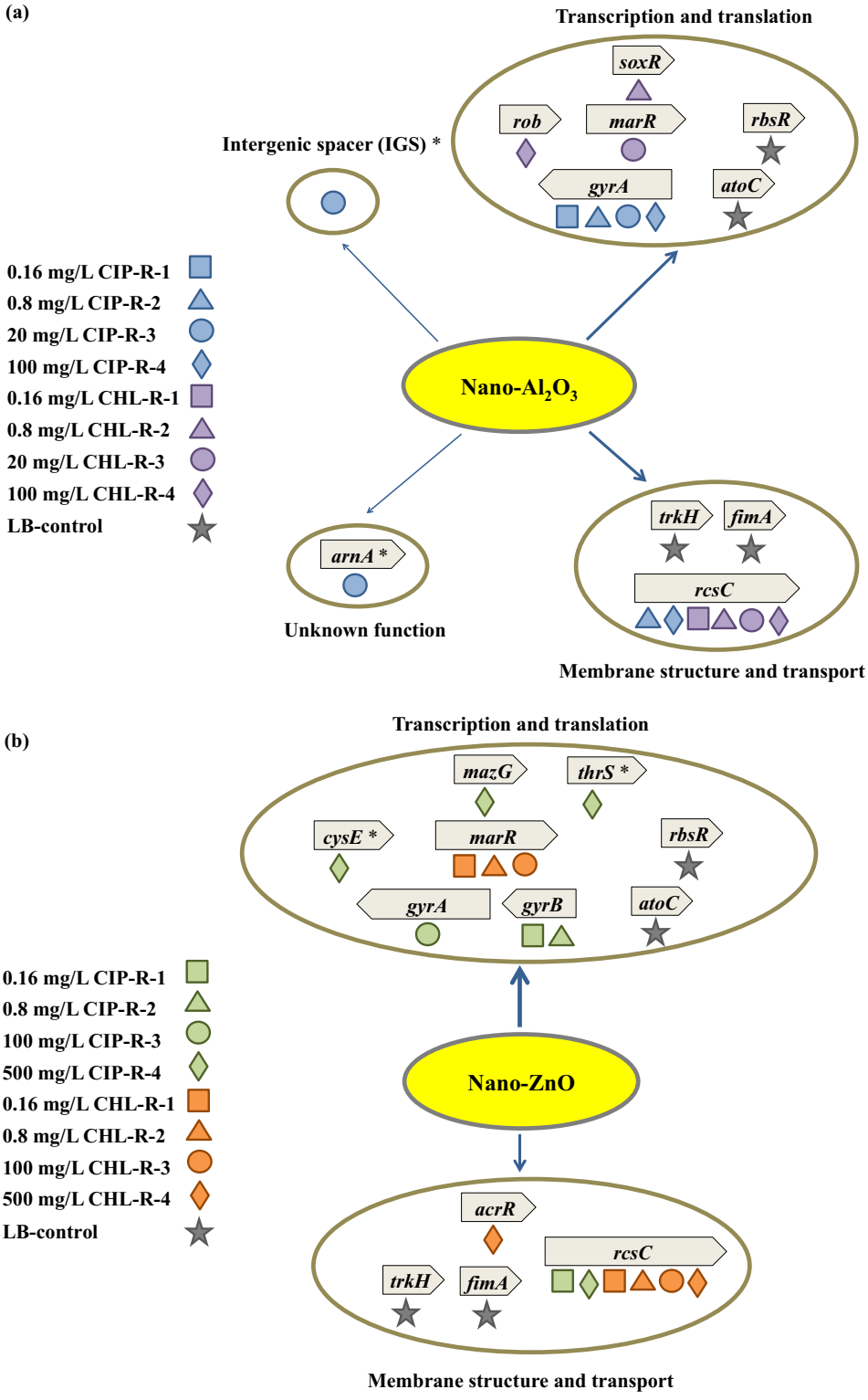

Fig. 5. Comparison of genetic changes identified in resistant mutation isolates induced by nano-Al_2O_3 (a) and nano-ZnO (b). Four individual resistant isolates from LB plates with CIP and CHL were shown by four different symbols and are color-coded to differentiate nano-Al_2O_3 and nano-ZnO. (a) Genetic changes identified in antibiotic resistant strains evolved under exposure to nano-Al_2O_3 were categorized into four major functional groups for: (i) membrane structure and transport, (ii) transcription and translation, (iii) intergenic spacer (IGS), and (iv) unknown functions. (b) Genetic changes identified in antibiotic resistant strains evolved under exposure to nano-ZnO were categorized into three major functional groups for: (i) membrane structure and transport, (ii) transcription and translation. Genetic changes identified in this study that have not been reported to play roles in antibiotic resistance were marked with *. The detailed information on these identified genetic changes was summarized in Tables S8–10. (For interpretation of the references to color in this figure legend, the reader is referred to the web version of this article.)

expression involved in oxidative stress and SOS response were to a much less extent compared with those induced by nano-Al_2O_3 and nano-ZnO (Fig. 2).

Previous evidences have proved that antibiotics (Kohanski et al., 2010), disinfection by-products (Lv et al., 2014; Li et al., 2016), and disinfectants (Chapman, 2003) can activate ROS-mediated oxidative stress and SOS response, consequently simulating mutagenesis and emerging of antimicrobial resistance (Andersson and Hughes, 2014; Kohanski et al., 2010). Here, we provided evidence that in addition to the above-mentioned chemicals, NMOs are also able to raise intracellular ROS production, induce oxidative stress and SOS response pathways, and therefore have the potential to induce antibiotic resistance.

3.2. NMOs exposure leads to antibiotic resistance phenotype

To verify the hypothesis that NMOs lead to antimicrobial resistance, the mutation frequencies of antibiotic resistance were firstly

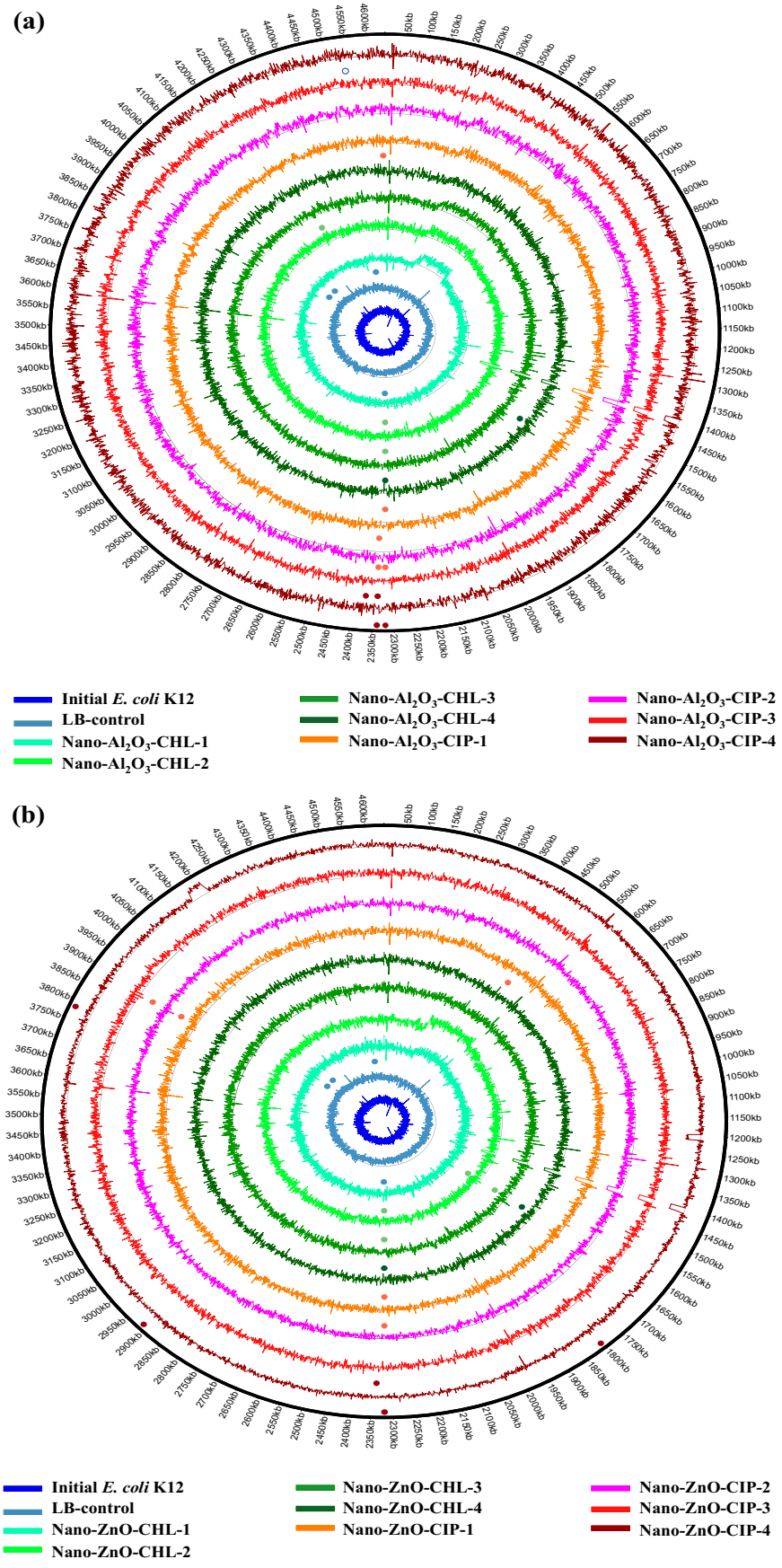

Fig. 6. Comparison of genome coverage and mutations distributed along the genomes among evolved antibiotic-resistant mutants induced by nano-Al_2O_3 (a) and nano-ZnO (b), initial *E. coli* K12 and control. Sequencing coverage of each strain was plotted using different color line, and the corresponding deep gray line in each Ring represented its average coverage. Solid dots and hollow dots indicated the SNP/InDel occurred in gene and the intergenic spacer (IGS), respectively. In addition, synonymous mutation occurred in gene was not shown in this figure. The detailed information of mutations was shown in Tables S8–10.

determined following exposure to NMOs and corresponding ions, as well as the untreated control group, respectively. The spontaneous resistance mutation frequencies in the untreated wild-type *E. coli* were approximately 10^{-8}–10^{-9} mutations/cell for different antibiotics (at 1 × MIC, as shown in Table S3), which are consistent with previous findings (Li et al., 2016; Firsov et al., 2000; CLSI, 2015). Both nano-Al_2O_3 and nano-ZnO treatment led to significant increases in the induction of CIP- and CHL-resistant mutations compared with those in the control groups (ANOVA, $P < 0.05$) (Fig. 3a–b and Table S5). The mutation frequencies of resistance to TET, GEN, AMP, and ERY were slightly increased, but < 2-fold increase compared to those in the control group, which was considered as non-clinically significance (Li et al., 2016; CLSI, 2015).

Both two types of NMOs resulted in concentration-dependent changes in resistance mutation frequency for two specific antibiotics, namely CIP and CHL, compared with those in the control groups (Fig. 3a–b and Table S5), however with different trends. Nano-ZnO treatments led to consistent increase in mutation frequencies for CIP and CHL resistance as concentrations inclined (Fig. 3b and Table S5). In contrast, the highest concentration of nano-Al_2O_3 showed sudden drop in the fold changes in mutation frequency for both CIP- and CHL-resistance (Fig. 3a and Table S5), which may be caused by the lethal effects and sudden increase of intracellular ROS formation at 500 mg/L of nano-Al_2O_3 (Fig. 1a).

Al^{3+} and Zn^{2+} might play weaker roles in the induction of resistant mutations, as indicated by the comparison of about 2-fold increase in mutation frequencies in exposure to Zn^{2+} and Al^{3+} ions compared to those with their NMOs (Fig. 3c and d, and Table S5), which might be due to the slight increase in ROS generation induced by Al^{3+} and Zn^{2+} (Fig. 1c–d). The released metal ion is generally recognized as an important contributor to the toxic behavior of dissolved nanoparticles (Misra et al., 2012). The released Zn^{2+} is believed to account for the toxicity of nano-ZnO, and our study was carried out based on 16–40% Zn^{2+} released from nano-ZnO (Yu et al., 2013; Song et al., 2010; Xu et al., 2016; Benavides et al., 2016). Previous studies could not detect Al^{3+} in the supernatant of nano-Al_2O_3, and here, we hypothesized 38–95% Al^{3+} released from nano-Al_2O_3 (Benavides et al., 2016; Sadiq et al., 2011).

Statistically significant positive correlations between fold changes in the mutation frequency of the CIP- and CHL-resistant mutations and ROS generation levels were observed for both NMOs treatments (Fig. 3e). However, there were no significant correlations between the changes in mutation frequencies of resistance and ROS formation after exposure to Al^{3+} and Zn^{2+} (data not shown). The slopes of the correlation curves varied among the different NMOs and resistance types, reflecting the various resistance mechanisms attributed to different antibiotics (Alekshun and Levy, 2007). To further confirm whether NMO-induced ROS was involved in promoting resistance mutagenesis, a potent hydroxyl radical scavenger test with thiourea (CH_4N_2S, TU) was performed (Text S6) (Kohanski et al., 2010; Zhang et al., 2017). The results showed that the mutation frequencies of CIP- and CHL-resistant *E. coli* following the addition of TU significantly decreased to the levels of the control group (Fig. S3). Hence, it is concluded that the accumulation of antibiotic resistance was highly related to intracellular ROS generated by nano-Al_2O_3 and nano-ZnO.

The MICs of the CIP- and CHL-resistant mutational strains induced by NMOs and corresponding ions were determined against six antibiotics (Figs. 4 and S4, Tables S6–7). As shown in Fig. 4, the NMO-induced mutational strains exhibited significant resistance to CIP and CHL, with 2–3-fold increase in MICs compared with that in the original wild-type *E. coli* strain (Tables S6–7). The induced CIP- and CHL-resistant strains simultaneously exhibited resistance to multiple antibiotics, including AMP (a β-lactam antibiotic), TET (a tetracycline antibiotic), and GEN (an aminoglycoside antibiotic) (Fig. 4). Al^{3+}- and Zn^{2+}-induced resistant mutant strains also displayed multiple-antibiotic resistance (Fig. S4 and Tables S6–7). Surprisingly, the MICs of NMO-induced mutant strains against antibiotics were a bit higher than that of the control group (spontaneous mutations), which indicated that the mutations in the host chromosome had the properties of both randomness and uncertainty (Lv et al., 2014; Flandrois et al., 2014). In spite of this, NMOs increased the mutation frequencies significantly, resulting in the enhanced development of antimicrobial resistance. Furthermore, the accumulation of mutations stimulated by NMO-induced oxidative stress might increase resistance levels to antibiotics.

3.3. The hereditary stability of resistance induced by NMOs

The hereditary stability of antibiotic resistance acquired upon exposure to NMOs is of great importance for public health and environmental safety. This study tested the changes in MICs of antibiotics resistant mutants after 5 cub-culture cycles in LB media over 5 days. The results provided clear evidence that the resistant mutants had good hereditary stability (Figs. S5–6 and Tables S6–7). Owing to the constant survival and adaptive evolution of resistant mutant pathogens, the stable hereditary characteristics of NMO-induced multiple-antibiotic resistance mutants certainly would aggravate the antibiotic resistance issues in the environment and pose potential public health issues (Andersson, 2003; Zhang et al., 2011).

3.4. Genetic insights in the multiple-antibiotic resistance induced by NMOs

To identify the genetic mutations responsible for multiple-antibiotic resistance, 16 isogenic clones resistant to CIP and CHL randomly picked from the population treated by NMOs (8 clones from nano-Al_2O_3 treatments and 8 from nano-ZnO treatments), one from the LB-control stain, and one from the original wild-type strain were subjected to whole-genome sequencing analysis. Four different SNPs were respectively identified on *atoC*, *rbsR*, *trkH*, and *fimA* genes in the LB-control clone, indicating their possible association with spontaneous mutations during selection and identification processes (i.e., culturing conditions and possible stress) (Table S8). Fifteen genetic mutations in 7 genes comprising 8 deletions and 7 SNPs were detected in 8 resistant *E. coli* strains induced by nano-Al_2O_3 (Fig. 5a and Tables S9–10). These genetic changes were associated with transcription and translation genes (*gyrA*, *rob*, *marR*, and *soxR*), membrane structure and transport genes (*rcsC*), unknown functions (*arnA*), and an intergenic spacer (IGS). Similarly, 16 genetic mutations in 8 genes comprising 2 insertions, 7 deletions, and 7 SNPs were detected in 8 resistant *E. coli* strains induced by nano-ZnO, which were associated with transcription and translation genes (*cysE*, *mazG*, *thrS*, *gyrA*, *gyrB*, and *marR*) and membrane structure and transport genes (*rcsC* and *acrR*) (Fig. 5b and Tables S9–10).

3.4.1. Genetic changes common to both NMOs

Both nano-Al_2O_3 and nano-ZnO induced genetic changes in *gryA*, *marR*, and *rcsC* genes (Figs. 5–6 and Tables S9–10). Three types of substitution mutations in the *gyrA* gene of CIP-resistant *E. coli* were stimulated by these two NMOs (Figs. 5–6 and Table S9). Previous findings proved that amino acid alternation in the *gyrA* and *gyrB* subunits of bacteria contributed to the resistance to quinolone antibiotics such as CIP (Lv et al., 2014; Li et al., 2016; Alekshun and Levy, 2007; Zhang et al., 2011). The three mutations in *gyrA* identified in the present study were likely to be associated with resistance to CIP (Figs. 5–6).

Four types of genetic changes in the multiple antibiotic resistance gene (*marR*) were identified, including a substitution mutation in the CHL-resistant mutant induced by nano-Al_2O_3, 1 insertion, 1 deletion, and 1 SNP in three different CHL-resistant mutants induced by nano-ZnO (Figs. 5–6 and Table S10). The *marR* gene is known to encode a negative auto-regulator of the *marRAB* operon, a regulatory region for controlling multiple-antibiotic resistance (Mar) in *E. coli* (Domain et al., 2007).

The same deletion of the A base at position 2,319,776 causing a

frameshift mutation in the *rcsC* gene was identified in 4 out of 8 total sequenced CIP-resistant strains induced by nano-Al_2O_3 and 8 total sequenced CHL-resistant strains induced by nano-ZnO (Figs. 5–6 and Tables S9–10). The two-component regulators *rcsB* and *rcsC* can negatively regulate the transcription of genes essential for capsular polysaccharide synthesis (Brill et al., 1988). Previous research showed that the observed increased capsular polysaccharides had the potential to protect *E. coli* from antibiotics, such as kanamycin, streptomycin, and AMP (Lu et al., 2008; Chin et al., 2014). Thus, the *rcsC* mutation might contribute to developing CIP resistance in *E. coli*.

3.4.2. Genetic changes specific to nano-Al_2O_3

The genetic changes in *soxR*, *rob*, *arnA*, and IGS were specifically induced by nano-Al_2O_3 (Figs. 5–6). Nano-Al_2O_3 induced a 4-base deletion at position 4,277,878 in *soxR* of one CIP-resistant *E. coli* and consequently resulted in a frameshift mutation (Figs. 5–6 and Table S9). A previous study revealed that the single-point-mutant SoxR proteins contribute to the multiple antibiotic resistance phenotypes of *E. coli* clinical isolates (Koutsolioutsou et al., 2005). The SoxR protein is expressed constitutively by oxidation and then transiently triggers transcription of the *soxS* gene, which can enhance SoxS protein to activate partial antibiotic resistance-regulated genes, such as *micF* and *acrAB* (Kabir and Shimizu, 2006).

A missense of C → T in base position 4,634,844 in the *rob* gene was found in one CHL-resistant clone induced by nano-Al_2O_3 (Figs. 5–6 and Table S10). The DNA-binding domain of Rob is a transcriptional activator belonging to the Xlys/AraC family and exhibits conjunction with MarA and SoxS for stimulation of the AcrAB efflux pump (Webber and Piddock, 2001; Fabrega et al., 2009). Few studies have reported that *E. coli* isolates harboring high resistance to levofloxacin (LEV) and CHL have mutations in *rob* genes (Toprak et al., 2012; Zayed et al., 2015).

A genomic deletion was identified in the IGS of one CIP-resistant *E. coli* induced by nano-Al_2O_3 (Figs. 5–6 and Table S9). IGSs, the sensitive markers of evolutionary change, refer to the zones of noncoding DNA sequences composed of a few nucleotides (Degnan et al., 2011). Base pair deletions or insertions in IGSs affect the various promoter functions and subsequent alteration of the initial stable complex with RNA polymerase of *E. coli*, which has been proven in some studies (Warne and deHaseth, 1993; Mulligan et al., 1985); however, little work has been conducted to date on the impacts of IGS sequence changes on antibiotic resistance.

3.4.3. Genetic changes specific to nano-ZnO

The mutations in *gyrB*, *mazG*, and *acrR* were specifically induced by nano-ZnO (Figs. 5–6 and Tables S9–10). Similar to the *gyrA* gene, mutations in the *gyrB* gene are also associated with antibiotic resistance. A frameshift mutation (GATT insert in base 2,910,048) occurred in the (d) NTP pyrophosphohydrolase-encoding *mazG* gene in a mutant induced by nano-ZnO, which could prevent mutations due to the misincorporation of non-canonical nucleotides into DNA (Lyu et al., 2013). It has been reported that mutations in the *mazG* gene are related to rifampin (RIF) resistance in *mycobacterium tuberculosis* (Lyu et al., 2013).

Another substitution mutation in the *acrR* gene was induced by nano-ZnO (Figs. 5–6 and Table S10). The AcrR protein acts as a local repressor of *acrAB* expression, being located upstream of the *acrA* gene yet transcribed in the contrary direction (Webber and Piddock, 2001; Fabrega et al., 2009). Few studies have reported that *E. coli* with mutations in the *acrA* and *rob* genes are highly resistant to LEV and CHL, respectively (Toprak et al., 2012; Zayed et al., 2015).

4. Environmental implications

In this study, the antimicrobial resistances induced by two NMOs, namely, nano-Al_2O_3 and nano-ZnO, were systematically investigated, and the results showed that these two NMOs could lead to enhanced mutations frequency and increases in multi-antibiotic resistance in the mutations compared to the controls. The mechanism underlying the induction of antimicrobial resistance by NMOs was also identified. Whole-genome sequencing analysis showed that the mutated genes correlated with mono- and multidrug resistance, as well as undetected resistance to antibiotics. Furthermore, NMOs significantly promoted intracellular ROS, which would lead to oxidative DNA damage and an error-prone SOS response, resulting in the increased frequency of antibiotic resistance mutagenesis.

Our results, for the first time, provided evidence and mechanistic insights show that NMOs could accelerate the mutagenesis and emergence of multiple resistances, which should be considered an important aspect of nanotoxicology and antimicrobial resistance. These findings raise the possibility that other emerging nanoparticles may also have risks associated with the occurrence of multiple-antibiotic resistance in clinical pathogens, which is of great importance for public health and environmental safety.

Notes

The authors declare no competing financial interest.

Acknowledgements

The content is solely the responsibility of the authors. This work was supported by grants from the National Natural Science Foundation of China (No. 21477024, 91643106, 21527814, and 21507012), United States National Science Foundation (NSF, CBET-1437257), the National Institute of Environmental Health Sciences (NIEHS) (PROTECT P42ES017198 and CRECE P50ES026049), and the Foundation of the Shanghai Key Laboratory of Chemical Assessment and Sustainablility (2017STCJ-04).

Appendix A. Supplementary data

Supplementary data to this article can be found online at https://doi.org/10.1016/j.envint.2018.10.030.

References

Alekshun, M.N., Levy, S.B., 2007. Molecular mechanisms of antibacterial multidrug resistance. Cell 128, 1037–1050.
Andersson, D.I., 2003. Persistence of antibiotic resistant bacteria. Curr. Opin. Microbiol. 6, 452–456.
Andersson, D.I., Hughes, D., 2014. Microbiological effects of sublethal levels of antibiotics. Nat. Rev. Microbiol. 12, 465–478.
Aruguete, D.M., Kim, B., Hochella, M.F., Ma, Y.J., Cheng, Y.W., Hoegh, A., Liu, J., Pruden, A., 2013. Antimicrobial nanotechnology: its potential for the effective management of microbial drug resistance and implications for research needs in microbial nanotoxicology. Environ. Sci.: Processes Impacts 15, 93–102.
Baharoglu, Z., Mazel, D., 2011. Vibrio cholerae triggers SOS and mutagenesis in response to a wide range of antibiotics: a route towards multiresistance. Antimicrob. Agents Chemother. 55, 2438–2441.
Baharoglu, Z., Krin, E., Mazel, D., 2013. RpoS plays a central role in the SOS induction by sub-lethal aminoglycoside concentrations in *Vibrio cholerae*. PLoS Genet. 9, e1003421.
Beaber, J.W., Hochhut, B., Waldor, M.K., 2004. SOS response promotes horizontal dissemination of antibiotic resistance genes. Nature 427, 72–74.
Benavides, M., Fernandez-Lodeiro, J., Coelho, P., Lodeiro, C., Diniz, M.S., 2016. Single and combined effects of aluminum (Al_2O_3) and zinc (ZnO) oxide nanoparticles in a freshwater fish, *Carassius auratus*. Environ. Sci. Pollut. Res. 23, 24578–24591.
Brill, J.A., Quinlan-Walshe, C., Gottesman, S., 1988. Fine-structure mapping and identification of two regulators of capsule synthesis in *Escherichia coli* K-12. J. Bacteriol. 170, 2599–2611.
Chalew, T.E.A., Ajmani, G.S., Huang, H.O., Schwab, K.J., 2013. Evaluating nanoparticle breakthrough during drinking water treatment. Environ. Health Perspect. 121, 1161–1166.
Chapman, J.S., 2003. Disinfectant resistance mechanisms, cross-resistance, and co-resistance. Int. Biodeterior. Biodegrad. 51, 271–276.
Chen, R., Huo, L.L., Shi, X.F., Bai, R., Zhang, Z.J., Zhao, Y.L., Chang, Y.Z., Chen, C.Y., 2014. Endoplasmic reticulum stress induced by zinc oxide nanoparticles is an earlier biomarker for nanotoxicological evaluation. ACS Nano 8, 2562–2574.
Chin, Y.P., Chang, S.F., Tseng, C.C., Chen, M.C., 2014. *Escherichia coli* capsular

polysaccharide synthesis, antibiotic susceptibility, and red blood cell agglutination. J. Exp. Clin. Med. 6, 16–20.
Clinical and Laboratory Standards Institute (CLSI), 2015. Performance Standards for Antimicrobial Susceptibility Testing; Twenty-fifth Informational Supplement M100-S25. Clinical and Laboratory Standards Institute, Wayne, PA.
Degnan, P.H., Ochman, H., Moran, N.A., 2011. Sequence conservation and functional constraint on intergenic spacers in reduced genomes of the obligate symbiont buchnera. PLoS Genet. 7, e1002252.
Ding, C.S., Pan, J., Jin, M., Yang, D., Shen, Z.Q., Wang, J.F., Zhang, B., Liu, W.L., Fu, J.L., Guo, X., Wang, D.N., Chen, Z.L., Yin, J., Qiu, Z.G., Li, J.W., 2016. Enhanced uptake of antibiotic resistance genes in the presence of nanoalumina. Nanotoxicology 10, 1051–1060.
Domain, F., Bina, X.R., Levy, S.B., 2007. Transketolase A, an enzyme in central metabolism, derepresses the marRAB multiple antibiotic resistance operon of *Escherichia coli* by interaction with MarR. Mol. Microbiol. 66, 383–394.
Fabrega, A., Madurga, S., Giralt, E., Vila, J., 2009. Mechanism of action of and resistance to quinolones. Microb. Biotechnol. 2, 40–61.
Firsov, A.A., Zinner, S.H., Iyu, L., Vostrov, S.N., 2000. Gemifloxacin and ciprofloxacin pharmacodynamics in an in-vitro dynamic model: prediction of the equivalent AUC/MIC breakpoints and doses. Int. J. Antimicrob. Agents 16 (4), 407–414.
Flandrois, J.P., Lina, G., Dumitrescu, O., 2014. MUBII-TB-DB: a database of mutations associated with antibiotic resistance in *Mycobacterium tuberculosis*. BMC Bioinf. 15, 107.
Gottschalk, F., Sonderer, T., Scholz, R.W., Nowack, B., 2009. Modeled environmental concentrations of engineered nanomaterials (TiO2, ZnO, Ag, CNT, Fullerenes) for different regions. Environ. Sci. Technol. 43, 9216–9222.
Gou, N., Onnis-Hayden, A., Gu, A.Z., 2010. Mechanistic toxicity assessment of nanomaterials by whole-cell-array stress genes expression analysis. Environ. Sci. Technol. 44, 5964–5970.
Gupta, S.C., Singh, R., Pochampally, R., Watabe, K., Mo, Y.Y., 2014. Acidosis promotes invasiveness of breast cancer cells through ROS-AKT-NF-kappaB pathway. Oncotarget 5, 12070–12082.
Gutierrez, A., Laureti, L., Crussard, S., Abida, H., Rodriguez-Rojas, A., Blazquez, J., Baharoglu, Z., Mazel, D., Darfeuille, F., Vogel, J., Matic, I., 2013. Beta-lactam antibiotics promote bacterial mutagenesis via an RpoS-mediated reduction in replication fidelity. Nat. Commun. 4, 1610.
Hajipour, M.J., Fromm, K.M., Ashkarran, A.A., Jimenez De Aberasturi, D., de Larramendi, I.R., Rojo, T., Serpooshan, V., Parak, W.J., Mahmoudi, M., 2012. Antibacterial properties of nanoparticles. Trends Biotechnol. 30, 499–511.
Hocquet, D., Llanes, C., Thouverez, M., Kulasekara, H.D., Bertrand, X., Plesiat, P., Mazel, D., Miller, S.I., 2012. Evidence for induction of integron-based antibiotic resistance by the SOS response in a clinical setting. PLoS Pathog. 8, e1002778.
Hristozov, D., Gottardo, S., Semenzin, E., Oomen, A., Bos, P., Peijnenburg, W., van Tongeren, M., Nowack, B., Hunt, N., Brunelli, A., Scott-Fordsmand, J.J., Tran, L., Marcomini, A., 2016. Frameworks and tools for risk assessment of manufactured nanomaterials. Environ. Int. 95, 36–53.
Kabir, M.M., Shimizu, K., 2006. Investigation into the effect of soxR and soxS genes deletion on the central metabolism of *Escherichia coli* based on gene expressions and enzyme activities. Biochem. Eng. J. 30, 39–47.
Kalyanaraman, B., Darley-Usmar, V., Davies, K.J., Dennery, P.A., Forman, H.J., Grisham, M.B., Mann, G.E., Moore, K., Roberts 2nd, L.J., Ischiropoulos, H., 2012. Measuring reactive oxygen and nitrogen species with fluorescent probes: challenges and limitations. Free Radic. Biol. Med. 52, 1–6.
Kohanski, M.A., Depristo, M.A., Collins, J.J., 2010. Sublethal antibiotic treatment leads to multidrug resistance via radical-induced mutagenesis. Mol. Cell 37, 311–320.
Koutsolioutsou, A., Pena-Llopis, S., Demple, B., 2005. Constitutive soxR mutations contribute to multiple-antibiotic resistance in clinical *Escherichia coli* isolates. Antimicrob. Agents Chemother. 49, 2746–2752.
Larsson, D.G.J., Andremont, A., Bengtsson-Palme, J., Brandt, K.K., de Roda Husman, A.M., Fagerstedt, P., Fick, J., Flach, C.F., Gaze, W.H., Kuroda, M., Kvint, K., Laxminarayan, R., Manaia, C.M., Nielsen, K.M., Plant, L., Ploy, M.C., Segovia, C., Simonet, P., Smalla, K., Snape, J., Topp, E., van Hengel, A.J., Verner-Jeffreys, D.W., Virta, M.P.J., Wellington, E.M., Wernersson, A.S., 2018. Critical knowledge gaps and research needs related to the environmental dimensions of antibiotic resistance. Environ. Int. 117, 132–138.
Lee, W.C., Li, L.C., Chen, J.B., Chang, H.W., 2015. Indoxyl sulfate-induced oxidative stress, mitochondrial dysfunction, and impaired biogenesis are partly protected by vitamin C and N-acetylcysteine. Sci. World J. 2015, 620826.
Li, D., Zeng, S., He, M., Gu, A.Z., 2016. Water disinfection byproducts induce antibiotic resistance-role of environmental pollutants in resistance phenomena. Environ. Sci. Technol. 50, 3193–3201.
Liu, C., Xie, X., Zhao, W., Yao, J., Kong, D., Boehm, A.B., Cui, Y., 2014. Static electricity powered copper oxide nanowire microbicidal electroporation for water disinfection. Nano Lett. 14, 5603–5608.
Lu, E., Trinh, T., Tsang, T., Yeung, J., 2008. Effect of growth in sublethal levels of kanamycin and streptomycin on capsular polysaccharide production and antibiotic resistance in *Escherichia coli* B23. J. Exp. Microbiol. Immunol. 12, 21–26.
Lv, L., Jiang, T., Zhang, S.H., Yu, X., 2014. Exposure to mutagenic disinfection byproducts leads to increase of antibiotic resistance in *Pseudomonas aeruginosa*. Environ. Sci. Technol. 48, 8188–8195.
Lyu, L.D., Tang, B.K., Fan, X.Y., Ma, H., Zhao, G.P., 2013. Mycobacterial MazG safeguards genetic stability via housecleaning of 5-OH-dCTP. PLoS Pathog. 9, e1003814.
Misra, S.K., Dybowska, A., Berhanu, D., Luoma, S.N., Valsami-Jones, E., 2012. The complexity of nanoparticle dissolution and its importance in nanotoxicological studies. Sci. Total Environ. 438, 225–232.
Mulligan, M.E., Brosius, J., McClure, W.R., 1985. Characterization in vitro of the effect of spacer length on the activity of *Escherichia coli* RNA polymerase at the TAC promoter. J. Biol. Chem. 260, 3529–3538.
Pelgrift, R.Y., Friedman, A.J., 2013. Nanotechnology as a therapeutic tool to combat microbial resistance. Adv. Drug Deliv. Rev. 65, 1803–1815.
Qiao, M., Ying, G.G., Singer, A.C., Zhu, Y.G., 2018. Review of antibiotic resistance in China and its environment. Environ. Int. 110, 160–172.
Qiu, Z.G., Yu, Y.M., Chen, Z.L., Jin, M., Yang, D., Zhao, Z.G., Wang, J.F., Shen, Z.Q., Wang, X.W., Qian, D., Huang, A.H., Zhang, B.C., Li, J.W., 2012. Nanoalumina promotes the horizontal transfer of multiresistance genes mediated by plasmids across genera. Proc. Natl. Acad. Sci. U. S. A. 109, 4944–4949.
Rosche, W.A., Foster, P.L., 2000. Determining mutation rates in bacterial populations. Methods 20, 4–17.
Sadiq, I.M., Pakrashi, S., Chandrasekaran, N., Mukherjee, A., 2011. Studies on toxicity of aluminum oxide (Al_2O_3) nanoparticles to microalgae species: *Scenedesmus* sp. and *Chlorella* sp. J. Nanopart. Res. 13, 3287–3299.
Seabra, A.B., Duran, N., 2015. Nanotoxicology of metal oxide nanoparticles. Metals 5, 934–975.
Song, W.H., Zhang, J.Y., Guo, J., Zhang, J.H., Ding, F., Li, L.Y., Sun, Z.T., 2010. Role of the dissolved zinc ion and reactive oxygen species in cytotoxicity of ZnO nanoparticles. Toxicol. Lett. 199, 389–397.
Tong, T.Z., Shereef, A., Wu, J.S., Binh, C.T.T., Kelly, J.J., Gaillard, J.F., Gray, K.A., 2013. Effects of material morphology on the phototoxicity of nano-TiO_2 to bacteria. Environ. Sci. Technol. 47, 12486–12495.
Toprak, E., Veres, A., Michel, J.B., Chait, R., Hartl, D.L., Kishony, R., 2012. Evolutionary paths to antibiotic resistance under dynamically sustained drug selection. Nat. Genet. 44, 101–105.
Vikesland, P.J., Pruden, A., Alvarez, P.J.J., Aga, D., Burgmann, H., Li, X.D., Manaia, C.M., Nambi, I., Wigginton, K., Zhang, T., Zhu, Y.G., 2017. Toward a comprehensive strategy to mitigate dissemination of environmental sources of antibiotic resistance. Environ. Sci. Technol. 51, 13061–13069.
World Health Organization (WHO), 2014. Antimicrobial Resistance: Global Report on Surveillance.
Warne, S.E., deHaseth, P.L., 1993. Promoter recognition by *Escherichia coli* RNA polymerase. Effects of single base pair deletions and insertions in the spacer DNA separating the -10 and -35 regions are dependent on spacer DNA sequence. Biochemistry 32, 6134–6140.
Waseem, A., Arshad, J., Iqbal, F., Sajjad, A., Mehmood, Z., Murtaza, G., 2014. Pollution status of Pakistan: a retrospective review on heavy metal contamination of water, soil, and vegetables. Biomed. Res. Int. 2014, 1–29 813206.
Webber, M.A., Piddock, L.J.V., 2001. Absence of mutations in marRAB or soxRS in acrB-overexpressing fluoroquinolone-resistant clinical and veterinary isolates of *Escherichia coli*. Antimicrob. Agents Chemother. 45, 1550–1552.
Xu, Y., Wang, C., Hou, J., Dai, S.S., Wang, P.F., Miao, L.Z., Lv, B.w., Yang, Y.Y., You, G.X., 2016. Effects of ZnO nanoparticles and Zn(2+) on fluvial biofilms and the related toxicity mechanisms. Sci. Total Environ. 544, 230–237.
Yu, K.N., Yoon, T.J., Minai-Tehrani, A., Kim, J.E., Park, S.J., Jeong, M.S., Ha, S.W., Lee, J.K., Kim, J.S., Cho, M.H., 2013. Zinc oxide nanoparticle induced autophagic cell death and mitochondrial damage via reactive oxygen species generation. Toxicol. in Vitro 27, 1187–1195.
Zayed, A.A.F., Essam, T.M., Hashem, A.G.M., El-Tayeb, O.M., 2015. 'Supermutators' found amongst highly levofloxacin-resistant *E. coli* isolates: a rapid protocol for the detection of mutation sites. Emerg. Microbes. Infect. 4, e4.
Zhang, Q.C., Lambert, G., Liao, D., Kim, H., Robin, K., Tung, C.K., Pourmand, N., Austin, R.H., 2011. Acceleration of emergence of bacterial antibiotic resistance in connected microenvironments. Science 333, 1764–1767.
Zhang, Y., Gu, A.Z., He, M., Li, D., Chen, J.M., 2017. Subinhibitory concentrations of disinfectants promote the horizontal transfer of multidrug resistance genes within and across genera. Environ. Sci. Technol. 51, 570–580.
Zhang, Y., Gu, A.Z., Cen, T.Y., Li, X.Y., Li, D., Chen, J.M., 2018. Petrol and diesel exhaust particles accelerate the horizontal transfer of plasmid-mediated antimicrobial resistance genes. Environ. Int. 114, 280–287.
Zheng, X., Wu, R., Chen, Y., 2011. Effects of ZnO nanoparticles on wastewater biological nitrogen and phosphorus removal. Environ. Sci. Technol. 45, 2826–2832.